ACS chemical biology

ARTICLES

pubs.acs.org/acschemicalbiology

Mapping the Pro-Peptide of the *Schistosoma mansoni* Cathepsin B1 Drug Target: Modulation of Inhibition by Heparin and Design of Mimetic Inhibitors

Martin Horn,[†] Adéla Jílková,[†,‡] Jiří Vondrášek,[†] Lucie Marešová,[†] Conor R. Caffrey,[§] and Michael Mareš[†,*]

[†]Institute of Organic Chemistry and Biochemistry, Academy of Sciences of the Czech Republic, Flemingovo nam. 2, 16610 Prague, Czech Republic

[‡]Department of Biochemistry, Faculty of Science, Charles University in Prague, Hlavova 8, 12843 Prague, Czech Republic

[§]Sandler Center for Drug Discovery, California Institute for Quantitative Biosciences (QB3), University of California San Francisco, 1700 Fourth Street, San Francisco, California 94158, United States

Supporting Information

ABSTRACT: Blood flukes of the genus *Schistosoma* cause the disease schistosomiasis that infects over 200 million people worldwide. Treatment relies on just one drug, and new therapies are needed should drug resistance emerge. *Schistosoma mansoni* cathepsin B1 (SmCB1) is a gut-associated protease that digests host blood proteins as source of nutrients. It is under evaluation as a therapeutic target. Enzymatic activity of the SmCB1 zymogen is prevented by the pro-peptide that sterically blocks the active site until activation of the zymogen to the mature enzyme. We investigated the structure−inhibition relationships of how the SmCB1 pro-peptide interacts with the enzyme core using a SmCB1 zymogen model and pro-peptide-derived synthetic fragments. Two regions were identified within the pro-peptide that govern its inhibitory interaction with the enzyme core: an "active site region" and a unique "heparin-binding region" that requires heparin. The latter region is apparently only found in the pro-peptides of cathepsins B associated with the gut of trematode parasites. Finally, using the active site region as a template and a docking model of SmCB1, we designed a series of inhibitors mimicking the pro-peptide structure, the best of which yielded low micromolar inhibition constants. Overall, we identify a novel glycosaminoglycan-mediated mechanism of inhibition by the pro-peptide that potentially regulates zymogen activation and describe a promising design strategy to develop antischistosomal drugs.

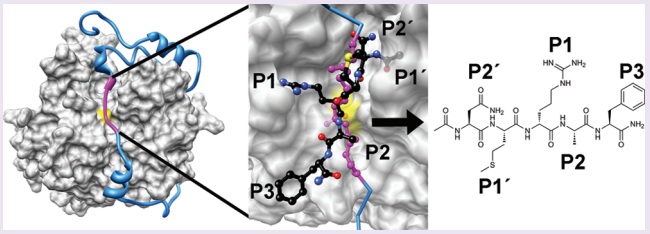

Schistosomiasis (bilharzia) is a chronic infectious disease that is caused by a trematode blood fluke and infects over 200 million people in tropical and subtropical areas.[1] Of the five species of schistosomes affecting humans, *Schistosoma mansoni* is a major agent of disease in the Middle East, Africa, and South America and the most convenient experimental model. Morbidity associated with the disease results from immuno-pathological reactions to parasite eggs trapped in various tissues, including the liver, intestinal tract, and bladder. Symptoms include decreased physical and cognitive performance, abdominal pain, and lassitude.[2] Treatment and control of schistosomiasis now relies on mass chemotherapy with just one drug, praziquantel, a tenuous situation should drug resistance emerge and spread.[1,3] Accordingly, there is pressure to identify new schistosomal protein targets for both chemo- and immuno-therapeutic interventions.

Adult schistosomes live in the cardiovascular system, and host blood proteins are a primary source of nutrients required for growth, development, and reproduction. In the schistosome gut, a network of proteases contributes to the digestion of host proteins to absorbable peptides and amino acids.[4,5] For *S. mansoni*, the component digestive proteases thus far characterized include (i) the Clan CA papain-like cathepsins B1 and L1, L2, and L3, dipeptidyl peptidase I (cathepsin C), (ii) the Clan CD asparaginyl endopeptidase (legumain), and (iii) the Clan AA aspartic protease, cathepsin D.[5−11] Similar acid pH-based proteolytic networks are found across phylogenetically diverse organisms such as nematodes, *Plasmodium* (malaria), and ticks.[12−15] Given their central importance to schistosome nutrition, therefore, gut proteases represent potential chemotherapeutic targets. The present research focuses on *S. mansoni* cathepsin B1 (SmCB1), which has been validated in a murine model of schistosomiasis mansoni as a molecular target for therapy with a peptidomimetic, vinyl sulfone protease inhibitor.[16] SmCB1 is a central digestive protease due first to its relative abundance and second to its complex proteolytic activity comprising both endopeptidase and exopeptidase (peptidyl dipeptidase) modes of action.[4,7]

Members of the Clan CA, Family C1 (papain-like) cysteine proteases,[17] including cathepsins B, are biosynthesized as inactive

Received: October 22, 2010
Accepted: March 4, 2011
Published: March 04, 2011

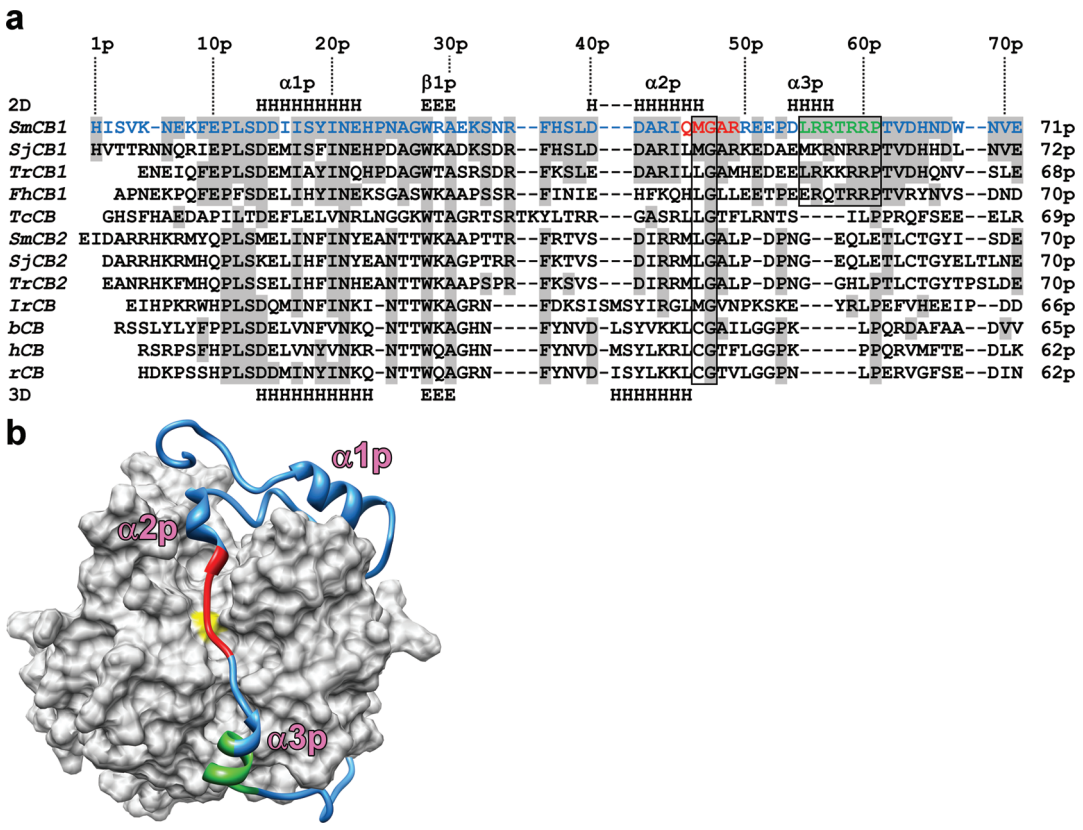

Figure 1. (a) Structure-based alignment of the pro-peptides of cathepsin B-type proteases from the human blood flukes *S. mansoni* (SmCB1 and SmCB2), *S. japonicum* (SjCB1 and SjCB2), the bird fluke *Trichobilharzia regenti* (TrCB1 and TrCB2), the liver fluke *Fasciola hepatica* (FhCB1), the protozoan *Trypanosoma cruzi* (TcCB), the tick *Ixodes ricinus* (IrCB), and bovine, human and rat cathepsins B (bCB, hCB and rCB; Uniprot accessions Q8MNY2, Q9SPM1, P43157, C7TYR4, Q4VRW9, A7L844, Q8I7B2, O61066, A4GTA7, P07688, P07858, and P00787, respectively). The secondary structure of the SmCB1 pro-peptide (2D) is based on prediction analysis, whereas the secondary structure of rCatB and hCatB pro-peptides (3D) is derived from crystallographic data (PDB entry 1MIR and 3PBH): H, α-helix; E, *β*-strand. The SmCB1 pro-peptide (blue) contains two inhibitory regions: an heparin-binding region (green) with a heparin-binding motif (boxed) and an active site region (red) containing residues in contact with the S1 and S1′ subsites of the active site (boxed). Residues identical with those of SmCB1 are shaded in gray; numbers above the alignment refer to the pro-peptide of SmCB1, the suffix "p" indicates pro-peptide numbering. A larger multiple alignment is provided in Supplementary Figure S1. (b) The tertiary structure of the SmCB1 zymogen was modeled using the X-ray structure of rat pro-cathepsin B (PDB entry 1MIR). The enzyme core is shown as a gray surface, and the active site Cys is in yellow. The pro-peptide (blue ribbon) contains two inhibitory regions color-coded as in the alignment (panel a): a heparin-binding region (residues 55p−61p in green) and an active site region (residues 45p−49p in red). The α-helices are indicated in magenta bold typeface.

zymogens (pro-cathepsins) in which the pro-peptide operates as an intramolecular inhibitor by blocking the active site. Activation to the mature, catalytically active forms occurs by proteolytic removal of the N-terminal pro-peptide (also termed the "activation peptide"); removal is either autocatalytic or involves other protease(s). After cleavage, the released pro-peptide can remain bound and inhibit its cognate enzyme.[18] The genomes of many organisms encode pro-peptide-like proteins that may act as intermolecular inhibitors of cysteine cathepsins.[19] Most studies on pro-peptide inhibition have been performed with full length pro-peptides and have demonstrated that inhibition of both parental and nonparental enzymes by pro-peptides is a function of the latter's structural complementarity.[20−23]

The application of pro-peptide fragments and crystal structures of cathepsin zymogens has shown that pro-peptides contain structural regions that govern their interactions with the mature enzyme.[24−30] As reported for the human cathepsin L pro-peptide, the structural principles defining pro-peptide inhibition can be used to construct small peptidomimetic inhibitors.[31] Also, studies with pro-peptides and their fragments have shown how they regulate the activity of cognate cysteine proteases from a diversity of protozoan and metazoan parasites including *Trypanosoma*, *Plasmodium*, and *Fasciola*[21,22,25,27] and, importantly, that they can suppress the development of *Plasmodium*.[28] Yet, there is a lack of detailed structure−activity studies for small pro-peptide mimetics of parasite peptidases and their potential as chemical starting points for therapeutic intervention of disease.

The activity of cysteine cathepsins is modulated by glycosaminoglycans (GAGs), sulfated polysaccharides with a strong negative charge that are widely distributed in tissues. The interaction of GAGs with mammalian cathepsins is complex and includes, for example, induction of collagenolytic activity of cathepsin K,[32] stabilization of cathepsin B at neutral pH,[33] and facilitation of autocatalytic activation of several cathepsins including cathepsins B, L, and S.[34−36] Mutation studies have shown that the GAG-accelerated activation involves interaction of GAGs with pro-peptides.[34,36] However, the effect of GAGs on inhibition by pro-peptides or their truncated synthetic derivatives has not been investigated.

Here, we define a structure−activity relationship (SAR) for SmCB1 and its pro-peptide. Using synthetic pro-peptide

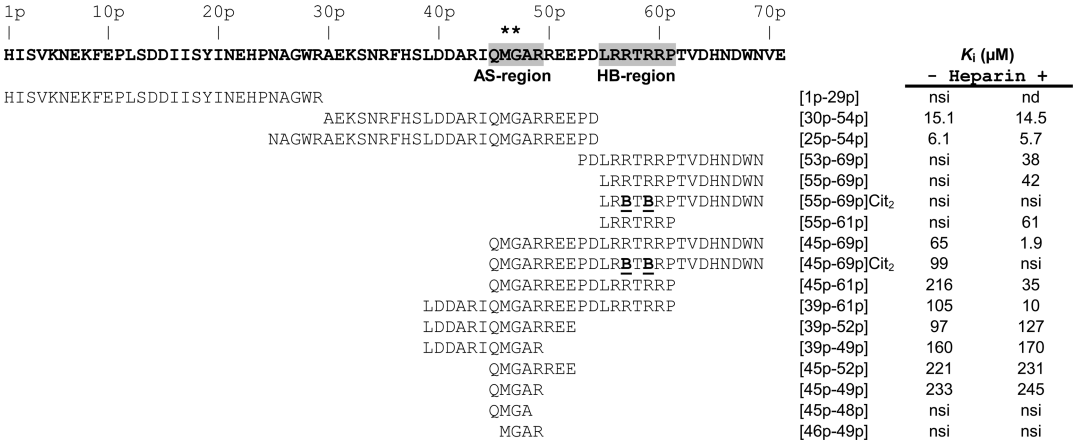

Figure 2. Design and inhibitory activity of synthetic peptide fragments derived from the pro-peptide of SmCB1. In the pro-peptide sequence, the active site (AS) and heparin-binding (HB) inhibitory regions are highlighted in gray, and those residues (Met46p and Gly47p) in contact with the S1 and S1′ subsites of the active site are marked (*). Synthetic peptide fragments are coded according to their location in the sequence; the suffix "p" indicates pro-peptide numbering. Substituted residues are in bold and underlined; B denotes citrulline. The inhibition constants (K_i) were determined in a kinetic activity assay with SmCB1 and the fluorogenic peptide substrate, Z-Phe-Arg-AMC, at pH 5.5 in the absence and presence of heparin. Mean values are given for triplicate measurements (SE values are within 10% of the mean); nsi, no significant inhibition with 400 μM peptide; nd, not determined due to low solubility.

fragments, we identify structural regions within the pro-peptide that account for its inhibition of the mature enzyme and uncover a new mechanism for their functional regulation by GAGs. In addition, one of these structural regions was employed as a scaffold to design small inhibitory peptides. These inhibitors of SmCB1 represent a chemical basis from which new antischistosomal drugs might be developed.

RESULTS AND DISCUSSION

SmCatB1 Pro-Peptide Contains a Phylogenetically Constrained α-Helix Incorporating a Heparin-Binding Motif. As the amino acid sequence of pro-SmCB1 (Uniprot accession Q8MNY2) is substantially homologous (48−57% identity) with those of mammalian pro-cathepsins B, we constructed a spatial model of the SmCB1 zymogen as a tool for structure−function analysis. We employed the X-ray structure of rat pro-cathepsin B (PDB entry 1MIR) as a template (Figure 1b). The SmCB1 pro-peptide comprises two α-helices (α1p and α2p) and a short β-strand (β1p) that is shared between zymogens of the cathepsin B subfamily. A significant difference occurs toward the C-terminal of the SmCB1 pro-peptide where there is an extra α-helical segment, denoted α3p. Figure 1a shows an alignment of pro-peptides of SmCB1 and other cathepsins B. The predicted secondary structure of α3p is associated with a sequence insertion that contains a consensus sequence for heparin binding, namely, XBBXBBX (where B is a basic amino acid and X is a hydropathic amino acid).[37] This new structural segment may be involved in intermolecular interactions between the SmCB1 pro-peptide and GAGs, as represented by heparin.

In addition, using blastp tools at NCBI, we inspected the cathepsin B-type sequences from other organisms and found that the predicted α3p helix including the heparin-binding motif is phylogenetically distributed in the pro-peptides of some, but not all, cathepsins B of parasitic trematodes, including *Schistosoma*, *Trichobilharzia*, and *Fasciola* spp. (Supplementary Figure S1). The feature is apparently absent from cathepsin B pro-peptides of nematodes, insects, and vertebrates. For those enzymes that contain the feature, the literature suggests they are gut localized and involved in digestion of host blood and/or tissues. By contrast, other trematode enzymes not associated with this function (*e.g.*, SmCB2, homologous to SmCB1 but found in the tegument (worm surface)), do not contain this structural feature.[38] Accordingly, it seems that α3p is a novel structural feature in the pro-peptide of SmCB1 and certain other cathepsins B involved in the digestion of host proteins by parasitic trematodes.

Design of Pro-Peptide Fragments for Structure−Inhibition Analysis. With the help of the 3D model (Figure 1), we designed a panel of peptide fragments derived from the sequence of the SmCB1 pro-peptide (Figure 2). The fragments were synthesized with capping groups (N-terminal acetyl and C-terminal amide) to mimic peptide linkages and to protect peptides against exopeptidase degradation by SmCB1. The main fragments were designed to reflect the secondary structure pattern, *i.e.*, the fragments [1p−29p], [30p−54p], and [53p−69p] contain α1p, α2p, and α3p α-helices, respectively. Fragment [25p−54p] combines α2p with the β-strand β1p that is involved in the formation of an adjacent hairpin structure. Met46p and Gly47p fill the S1′ and S1 pockets of the active site of SmCB1. Both Met46p and Gly47p are centrally positioned in a series of peptides that were synthesized to extend in both the N-terminal (to include α2p) and C-terminal directions (to include α3p and its heparin-binding motif, and the pro-peptide C-terminus). A number of the synthesized fragments contain sequence stretches that form α-helices according to the prediction analysis and the 3D model (Figures 1 and 2). For representative fragments, we demonstrated by circular dichroism spectroscopy the presence of a partial α-helical conformation (Supplementary Figure S2). This underscores the utility of the model and designed fragments to analyze structure−inhibition relationships in the SmCB1 pro-peptide.

Pro-Peptide Mapping of SmCB1 Identifies Two Inhibitory Regions with Differing Sensitivities to Heparin. The inhibition constants (K_i) for an array of synthetic pro-peptide fragments against mature SmCB1 was measured using a kinetic assay with the fluorogenic substrate Z-Phe-Arg-AMC (Figure 2).

The long N- and C-terminal pro-peptide fragments ([1p−29p] and [53p−69p]) did not inhibit SmCB1 activity. In contrast, the central fragment [25p−54p] had a K_i of 6 μM. The potency of the central fragment was partially supported by the β1p structure as demonstrated by its deletion in peptide [30p−54p] that resulted in a K_i of 15 μM. This β-strand contains the conserved hydrophobic residues Trp28p and Ala30p that interact with the "pro-peptide binding loop", a short loop found on the surface of the core of mammalian pro-cathepsins B.[29] The central fragment [30p−54p] that traverses the active site was gradually truncated at both termini in a set of peptides spanning the S and S′ subsites. The extensive trimming of the 25-mer peptide did not abolish inhibition but did result in increased K_i values up to 233 μM as measured for the shortest pentapeptide QMGAR [45p−49p]. This segment represents a minimal inhibitory region, the active site region, which surrounds Met46p−Gly47p residues occupying the S1′ and S1 subsites.

Next, we tested the inhibitory potency of the synthetic peptides in the presence of heparin, as the heparin-binding motif is located in the C-terminal region of the SmCB1 pro-peptide (residues 55p−61p). Interestingly, the large C-terminal fragment [53p−69p] required heparin to display inhibition, which was substantial (K_i = 38 μM; Figure 2). The same heparin-dependent inhibition was observed for the shorter peptide LRRTRRP [55p−61p] that is equivalent to the length of the heparin-binding motif (K_i = 61 μM in the presence of heparin). Accordingly, we identify a novel heparin-binding region [55p−61p] that acts as an inhibitor of SmCB1, but only in the presence of heparin.

The peptides spanning both the heparin-binding and active site regions ([45p−69p], [39p−61p], [45p−61p]) inhibited with K_i values in the range 65−216 μM in the absence of heparin. In the presence of heparin, however, these values were decreased by 1 order of magnitude (K_i ∼2−35 μM). This demonstrates that the heparin-binding region significantly improves the inhibitory potency of the active site region. The properties of the most potent peptide fragment [45p−69p] were studied in detail. First, the mode of inhibition was found to be competitive (Figure 3), which is consistent with the expected interaction of this peptide in the substrate-binding site through the active site region. Second, the inhibitory selectivity was investigated. It is known that pro-peptides of cysteine proteases and their truncated synthetic forms bind not just to the mature cognate enzymes but also to homologous enzymes with varying potencies (for a review, see ref 20). The pro-SmCB1 peptide [45p−69p] inhibited bovine cathepsin B with K_i values of 512 and 257 μM in the presence and absence of heparin, respectively. This compares with the K_i values for SmCB1 of 2 and 65 μM, respectively. The weaker inhibition of bovine cathepsin B activity can be explained by its partial homology (51% identity) to SmCB1. Importantly, heparin does not improve the inhibition of the mammalian enzyme by the peptide [45p−69p], pointing to the specificity of the interaction between SmCB1 and the fragment through the heparin-binding region.

Overall, mapping the pro-peptide of SmCB1 with synthetic peptides identifies two distinct small inhibitory regions. First, the active site region is topologically similar (*i.e.*, in contact with the active site residues) to pro-peptide fragments that inhibit other cysteine proteases, including mammalian cathepsin B.[24−26] In those reports, 7- to 15-mer peptides had K_i values in the range of those described here. For SmCB1, inhibition by peptides covering the active site region is independent of the presence

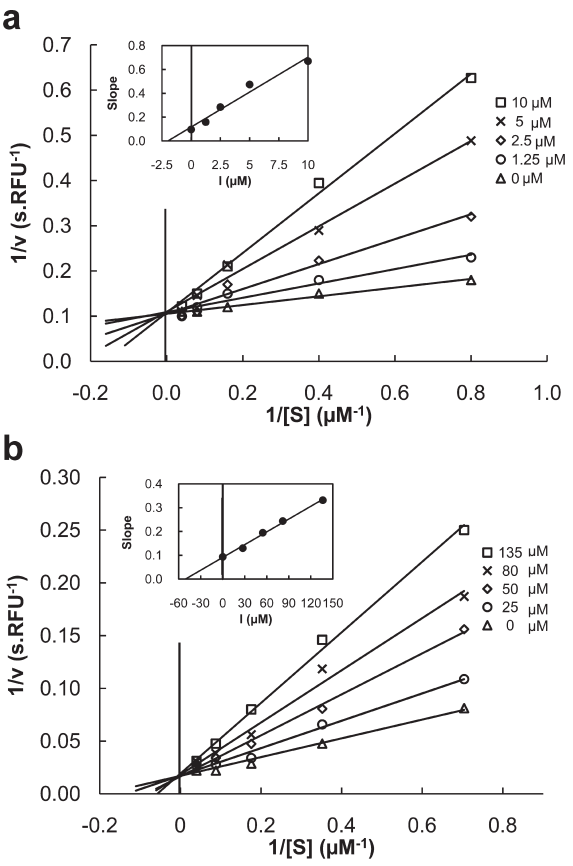

Figure 3. Competitive mode of inhibition of SmCB1 by fragments [45p−69p] (a) and [55p−61p] (b) derived from the SmCB1 pro-peptide. A Lineweaver−Burk plot is presented together with a secondary plot of the same data (inset); K_i values are 2.0 and 55 μM for [45p−69p] and [55p−61p], respectively. The activity assay with the fluorogenic peptidyl substrate, Z-Phe-Arg-AMC, was performed at pH 5.5 in the presence of 25 μg mL^{-1} heparin. Mean values are given for triplicate measurements (SE were within 10%).

or absence of heparin. Second, it is now clear that the heparin-binding region, unique to certain trematode cathepsins B, can also inhibit proteolysis by SmCB1, but that heparin (and possibly other GAGs) needs to be present.

Heparin Interacts with Both the Heparin-Binding Region of the Pro-Peptide and the Enzyme Core. The properties of the heparin-binding region's interaction with heparin were examined. For fragments [55p−69p] and [45p−69p], we synthesized derivatives in which the heparin-binding motif was altered by substituting two positively charged arginine residues with citrulline isosteres that possess uncharged side chains (peptides [55p−69p]Cit$_2$ and [45p−69p]Cit$_2$). This abolished the heparin-dependent inhibition of SmCB1 (Figure 2). The result was confirmed by heparin affinity chromatography (Figure 4): the wild-type peptide [45p−69p] bound to immobilized heparin, whereas its citruline derivative [45p−69p]Cit$_2$ did not.

In addition, mature, *i.e.*, fully activated, SmCB1 was bound by the heparin affinity column (Figure 4). This can be rationalized on the basis that SmCB1, being more basic then mammalian cathepsins B (theoretical pI values of 8.7 and 5.1, respectively), can interact with the positively charged heparin. The mature SmCB1 sequence does not contain a canonical heparin-binding

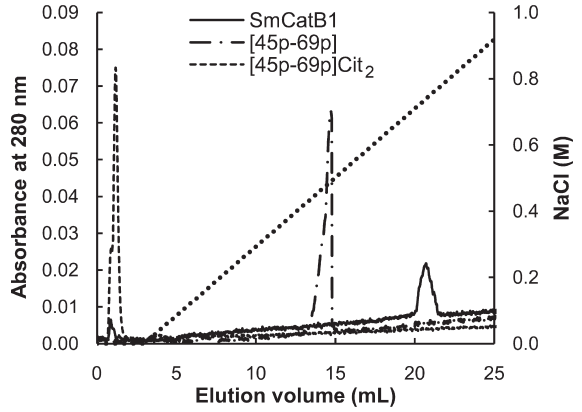

Figure 4. Heparin affinity chromatography of SmCB1, its pro-peptide-derived fragment [45p−69p] containing the heparin-binding motif, and the same fragment but in which the two positively charged arginine residues have been substituted with citrulline [45p−69p]Cit_2. The column was equilibrated in 25 mM sodium acetate, pH 5.5, and eluted with a linear gradient of 0−1 M NaCl.

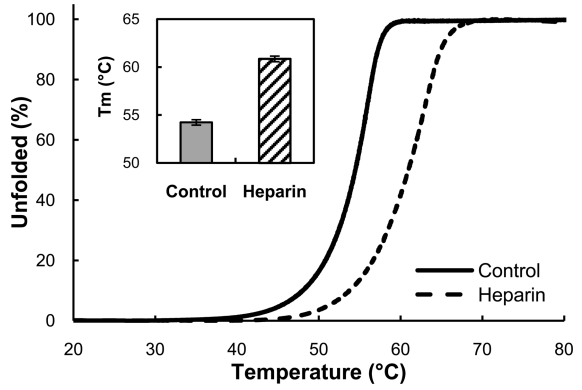

Figure 5. Thermal denaturation of SmCB1 using the thermofluor technique. The curves were recorded for SmCB1 in the presence (dashed line) and absence (solid line, control) of heparin (25 μg mL^{-1}). The fraction of unfolded protein is displayed. Inset: the melting temperature (T_m) values determined from the denaturation curves. Mean values ± SE are given for triplicate measurements.

motif; however, inspection of the 3D model reveals several positively charged patches. One of these involves the occluding loop on the "front site" surface of SmCB1 close to the active site (Supplementary Figure S3). Basic surface patches are reported to mediate heparin−protein interactions.[39] The interaction of SmCB1 with heparin was also studied using the thermofluor technique[40,41] in order to understand whether heparin alters the thermal stability of SmCB1. In the presence of heparin, the thermal stability of SmCB1 was increased (melting temperature (T_m) shifted from 54 to 61 °C (Figure 5)), thus indicating the formation of a complex between SmCB1 and heparin.

On the basis of the above results, we propose a mechanism by which heparin promotes the inhibitory functionality of the heparin-binding region. The heparin polymer interconnects the pro-peptide heparin-binding region through the heparin-binding motif and the enzyme core through a surface basic patch. This facilitates docking of the heparin-binding region in a proper orientation, which finally leads to steric hindrance of the adjacent active site by a bulky complex formed from the heparin-binding peptide and heparin. This is in line with the competitive mode of inhibition of SmCB1 by the synthetic heparin-binding region [55p−61p] in the presence of heparin (Figure 3b). The electrostatic character of the involved interactions is supported by the finding that the heparin-dependent inhibition of SmCB1 by [45p−69p] is abolished by 0.3 M NaCl (data not shown). The specific requirements for the heparin structure were tested using heparins ranging from 2 to 17 kDa in size. The inhibition by peptide [45p−69p] did not vary significantly (K_i ∼1.0−1.9 μM), demonstrating that a 2 kDa hexasaccharide fragment (K_i = 1.2 μM) is as effective as 17 kDa heparin (K_i = 1.9 μM) in mediating the interaction.

What is the function of the heparin-binding region? We speculate that it may participate in regulating the activation of the SmCB1 zymogen. For several mammalian cysteine cathepsins, including cathepsin B, it was reported that heparin and other GAGs accelerate zymogen autoactivation through destabilization of the pro-peptide interaction with the mature enzyme, thus facilitating its autocatalytic cleavage.[34,36] The present data suggest that the modulatory activities of GAGs are more complex. In the case of SmCB1, these polysaccharides might produce increased stabilization of the pro-peptide interaction *via* the heparin-binding region. GAGs are widespread in host tissues and are also found in *Schistosoma*.[42] Interestingly, and unlike mammalian cathepsins B, the SmCB1 zymogen only partially autoactivates and the assistance of processing proteases, such as an asparaginyl endopeptidase, is necessary for complete zymogen conversion.[7] The partially processed SmCB1 zymogen is catalytically inactive and still retains a pro-peptide fragment (residues 39p−71p) that includes both the active site and heparin-binding regions.[7] Our future research will test the hypothesis that GAGs regulate the activation of pro-SmCB1 using purified recombinant zymogen and various heparin-binding region mutants.

Pro-Peptide Mimetics Derived from the Active Site Region as a Design Basis for Novel Anti-Schistosomals. We found that the active site region [45p−49p] synthesized as a synthetic pentapeptide retains some inhibitory activity (K_i = 233 μM) against SmCB1 (Figure 2). Also, neither this pentapeptide nor variants extended in either the N- ([30p−54p]) or C-terminal directions ([45p−69p]) are hydrolyzed by SmCB1 (see Supplementary Figure S4). We suggest that the synthetic active site-directed pentapeptide likely binds in the same manner to the active site as the native pro-peptide, *i.e.*, in the opposite orientation than substrates, and thus prevents cleavage. Accordingly, we set out to use the active site region as a starting scaffold for the design of more potent inhibitors of SmCB1.

In our structure-based design, we employed a 3D model of mature active SmCB1 that was built by homology modeling using the X-ray structure of rat cathepsin B (PDB entry 1CPJ) as template (Figure 6). The wild-type pentapeptide [45p−49p], Ac-QMGAR, was docked into the active site cleft where it occupied the S2′ through S3 subsites. The corresponding P2′ through P3 residues in the inhibitor structure were substituted by L- and D-amino acids, and the modified structures were redocked and evaluated for their interaction potential. The best candidates selected *in silico* were synthesized. These compounds are listed in Table 1 together with their K_i values for SmCB1. Initially, we substituted the P1 residue (Gly) with D-Arg that is known to prevent interaction of peptidic ligands in the substrate-like binding mode.[31] Then, we used Phe at P3 to fill the S3 pocket of SmCB1 as bulky hydrophobic groups in this position are generally favored in SmCB1 substrates.[43] Next, the P2′ residue

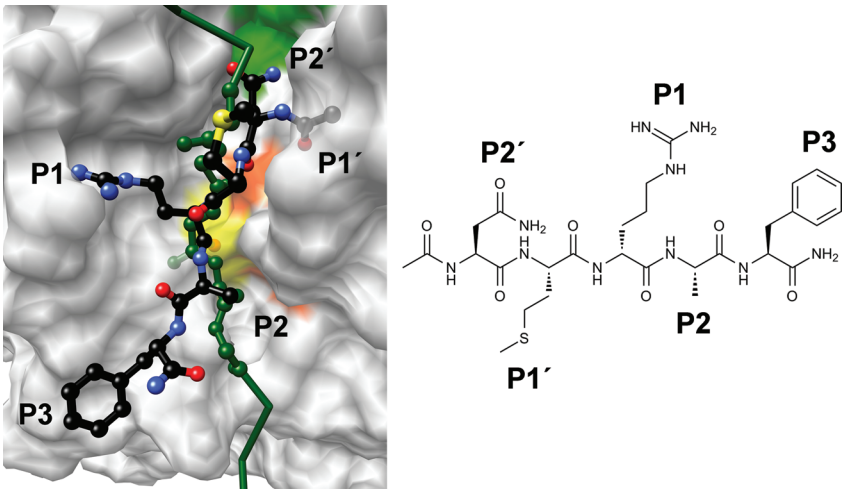

Figure 6. Chemical structure and docking model of the Ac-NMrAF inhibitor, a synthetic mimetic of the pro-peptide active site region. The inhibitor (black ball-and-stick) was docked into the active site of SmCB1 (gray surface) and residues in the P2′−P3 positions are indicated. The Ac-NMrAF binding mode is superimposed on that of the SmCB1 pro-peptide (dark green, with active site region backbone in ball-and-stick). Heteroatoms of Ac-NMrAF are colored red for oxygen, blue for nitrogen, and yellow for sulfur. In the SmCB1 active site, the catalytic residues Cys100 and His270 are highlighted in yellow and orange, respectively. The histidine residues of the occluding loop (His180 and His181) are in green. The SmCB1 molecule is oriented as in Figure 1.

that interacts with the occluding loop of SmCB1 was optimized. During this step, we also evaluated N-terminal capping, which for several P2′ substituents was required for efficient inhibition. This step defined two routes for the further iterative design of compounds containing either an acetylated P2′ Asn or an N-terminally free Glu. Finally, employing mostly hydrophobic residues at P1′ and P2 yielded Trp and Ala, respectively, as generally suitable substituents. In summary, the screening of 48 inhibitors (Table 1) yielded 5 inhibitors with K_i values lower than 50 μM and one (EYrAF) with a value of 14 μM, *i.e.*, 16-fold more potent than the native active site region [45p−49p] (K_i = 233 μM). The 5 best ranked inhibitors were also screened against human cathepsins B, L, and S under analogous conditions, and no significant inhibition was observed (Table 1).

Docking Ac-NMrAF, one of the more potent inhibitors (K_i = 32 μM), in the active site of SmCB1 (Figure 6) illustrates a network of potential interactions (contacts within 4 Å) that is formed between enzyme and inhibitor. These include P3 (Gly67, Leu68, Ile74), P2 (Gly72, Gly73), P1 (Gly27, Cys39, Cys70, Glu71, Ile122, His199), P1′ (Gly197, Gly198, Leu196), and P2′ (His110, Val176, Leu181, Leu196, Trp221). The P2′ residue (Ac-Asn) interacts with His110 of the occluding loop. A similar interaction of the epoxysuccinyl peptidyl inhibitor, CA-074, with His110 and His111 was critical for its potent inhibition of bovine cathepsin B.[44]

In conclusion, we demonstrate that the active site region is a useful starting scaffold in the design of inhibitors selective for SmCB1 over host-derived cathepsins B, L, and S. The K_i values of the most potent pentapeptide inhibitors are in the mid to low micromolar range and are thus an improvement on the inhibition produced by the original active site region [45p−49p]. Moreover, the K_i values are comparable with those measured for the large central 25-mer pro-peptide fragment [30p−54p] (Figure 2). We will continue the optimization process by introducing unnatural amino acids and building blocks. These modifications may confer low or submicromolar inhibition as was found for the pro-peptide-derived inhibitors of human cathepsin L.[31] We will also attempt to cocrystallize optimized inhibitors with SmCB1 for X-ray analysis to provide direct evidence for the modeled binding mode. This will further the rational design of inhibitors that may help identify molecules for consideration as antischistosomal drugs.

METHODS

Materials. Heparins from porcine intestinal mucosa with an average molecular weight of 17, 5, and 3 kDa were from Sigma, and heparin hexasaccharide was from Dextra Laboratories. The fluorogenic substrate Z-Phe-Arg-AMC was from Bachem. Amino acid precursors and resins for peptide synthesis were from Iris Biotech. *S. mansoni* asparaginyl endopeptidase (SmAE) was produced recombinantly in *Pichia pastoris* as described in ref 10. Bovine cathepsin B was purified from bovine spleen,[45] human cathepsin B was obtained from Merck, and human cathepsins L and S from Sigma.

Recombinant Expression and Purification of SmCB1. SmCB1 was expressed in the X33 strain of the methylotrophic yeast *P. pastoris* as described previously.[7] The induction media were concentrated and desalted on a Sephadex G-25 column equilibrated with 25 mM sodium acetate, pH 5.5. Recombinant protein (a mixture of zymogen and intermediate forms) was separated on a Mono S HR 5/5 column (GE Healthcare Bio-Sciences) equilibrated with 25 mM sodium acetate, pH 5.5 and eluted using a linear gradient of 0−1 M NaCl. The activated SmCB1 was obtained by proteolytic treatment with SmAE in 0.1 M sodium acetate, pH 5.0, containing 2.5 mM dithiothreitol.[7] The conversion to active SmCB1 was monitored using the Z-Phe-Arg-AMC assay (see below) and SDS-PAGE. SmCB1 was finally purified on a Mono S HR 5/5 column as above. The preparation was concentrated and desalted into 20 mM sodium acetate, pH 5.5 using Amicon Ultracel-10k (Millipore). The typical yield was 2 mg of SmCB1 from 1 L of induction media.

Synthesis of Peptides. Peptides were synthesized by Fmoc solid phase chemistry in an ABI 433A Peptide Synthesizer (Applied Biosystems) in the form of peptidyl amides with free or acetylated N-termini as described previously.[46] Peptides were purified by RP-HPLC over a C18 column using a trifluoroacetic acid (TFA) elution system and characterized by ESI mass spectrometry on an LCQ Classic

Table 1. Structure-Based Optimization of Synthetic Inhibitors Derived from the Active Site Region of the SmCB1 Pro-Peptide

peptide[a]	structure[b]	K_i (μM)[c] Ac	K_i (μM)[c] NH_2
	QMGARREE	221	268
	QMrARREE	83	159
	QMGAR	233	nsi
XMrAF	QMrAF	210	nsi
	NMrAF	32[d]	nsi
	EMrAF	nsi	161
	DMrAF	nsi	nsi
XWrAF	PWrAF	134	265
	HWrAF	159	nsi
	RWrAF	164	189
	QWrAF	266	291
	SWrAF	299	nsi
	TWrAF	nsi	66
NXrAF	NWrAF	22[d]	
	NYrAF	nsi	
	NFrAF	nsi	
EXrAF	EYrAF		14[d]
	EWrAF		37[d]
	ECrAF		97
	EFrAF		112
	EIrAF		177
	ELrAF		225
	EArAF		230
	EGrAF		240
	ESrAF		255
	EHrAF		nsi
	ERrAF		nsi
	ER(Tos)rAF		nsi
EMXAF	EMkAF		299
	EMVAF		nsi
	EMLAF		nsi
	EMFAF		nsi
EWXAF	EWwAF		46[d]
	EWiAF		nsi
	EWlAF		nsi
	EWfAF		nsi
EMrXF	EMrIF		231
	EMrFF		nsi
	EMrRF		nsi

[a] X positions (P2′−P3 residues) were substituted with the selected L- and D-amino acids (upper- and lower-case letters, respectively). [b] Peptides were synthesized as carboxy-amides with free (NH_2) or acetylated (Ac) N-termini; R(Tos), tosyl-arginine. [c] The inhibition constants (K_i) were determined in a kinetic activity assay with SmCB1 and the fluorogenic peptidyl substrate, Z-Phe-Arg-AMC. Mean values are given for triplicate measurements (SE values were within 10% of means); nsi, no significant inhibition with 300 μM peptide. [d] Peptides were screened against human cathepsins B, L, and S under conditions analogous to those used for SmCB1, and no significant inhibition was observed at a 300 μM peptide concentration.

Finnigan Mat device (Thermo Finnigan). The characterization of the synthesized peptides is presented in Supplementary Table S1.

SmCB1 Activity and Inhibition Assays. SmCB1 activity was measured with the fluorogenic substrate Z-Phe-Arg-AMC.[7] The reaction was performed in a 96-well microplate format in a total assay volume of 100 μL in 0.1 M sodium acetate, pH 5.5, containing 2 mM dithiothreitol and 0.1% (w/v) PEG 6000. For inhibition measurements, the enzyme (0.6 nM) was preincubated with synthetic peptide (0−400 μM) at 37 °C for 15 min followed by the addition of 25 μM Z-Phe-Arg-AMC. Where indicated, the 17 kDa heparin was added to the preincubation mixture to give a final concentration of 25 μg mL^{-1} in the assay; this value was selected based on the fact that the potential of heparin to promote the SmCB1 inhibition (by peptides [45p−69p] and [55p−61p]) did not vary significantly in the tested range of 0.5−50 μg mL^{-1} (data not shown). The kinetics of product release was continuously monitored in an Infinite M200 microplate reader (Tecan) at excitation and emission wavelengths of 360 and 465 nm, respectively. Each measurement was performed in triplicate. The inhibition constants (K_i) were determined from the residual velocities using the dose−response plot (v_i/v_0 vs [I]) to obtain IC_{50} values that were then converted to K_i values by Cheng and Prusoff relationships.[47] The inhibition mode was determined using an analogous activity assay and the initial velocities of product release were interpreted using the Lineweaver−Burk plot. The active site concentration of SmCB1 was determined by titration with E-64, and the peptide solutions were quantified by amino acid analysis. The same activity assay was employed with bovine and human cathepsins B and human cathepsins L and S.

Stability of Peptides. Resistance of pro-peptide-derived fragments to proteolysis was investigated as described previously[48] under conditions similar to those used in the inhibition assay. The reaction mixtures contained 0.6 or 6.0 nM SmCB1 and 100 μM synthetic peptide in 0.1 mM sodium acetate, pH 5.5, containing 2 mM dithiothreitol (and 25 μg mL^{-1} 17 kDa heparin where indicated). The reaction was incubated at 37 °C for 16 h and stopped by the addition of 10 μM E-64. Mixtures were analyzed by RP-HPLC, and the obtained profiles were compared to those of controls not subjected to enzyme treatment. The RP-HPLC separation was performed on a Vydac C18 column (218TP54, Vydac) equilibrated in 5% (v/v) acetonitrile solution in 0.1% (v/v) TFA and eluted with a 2% min^{-1} gradient of a 90% (v/v) acetonitrile solution in 0.1% (v/v) TFA.

Secondary Structure Prediction. Prediction of secondary structure was performed using the PORTER and PSIPRED web services (http://distill.ucd.ie/porter/ and http://bioinf.cs.ucl.ac.uk/psipred/).

Molecular Modeling. A model of SmCB1 was constructed using the X-ray structure of rat cathepsin B (PDB entry 1CPJ) as a template and a pairwise sequence alignment generated by the BLAST program using a BLOSUM62 substitution matrix. The homology module of the MOE program was used for the modeling of the SmCB1 structure.[49] The Ac-NMrAF inhibitor was built into the SmCB1 active site cleft based on the position of three known active site ligands: (i) Compound 13 inhibitor from the human cathepsin L complex (PDB entry 1MHW) defined the orientation in the P1 to P3 positions; (ii) CA-074 inhibitor from the bovine cathepsin B complex (PDB entry 1QDQ) defined the orientation in the P2′ position; and (iii) CGT (42p−44p) segment in the pro-peptide of rat pro-cathepsin B (PDB accession 1MIR) defined the orientation in the P1′−P2 positions. The conformation of Ac-NMrAF was refined by applying the LigX module of the MOE for the optimization procedure. The final binding mode of the inhibitor was selected by the best-fit model based on the London dG scoring function and the generalized Born method.[50] The same strategy was used for the docking of other compounds derived from the active site region to evaluate their interaction potential with SmCB1. The structure of pro-SmCB1 was modeled on the basis of the X-ray structure of the rat pro-cathepsin B (PDB accession 1MIR) as template as described for the SmCB1 model. The multiple sequence alignment of the pro-peptide segments that was used for the SmCB1 modeling was generated by ClustalW2 (Figure 1a). Molecular images were generated with UCSF Chimera (http://www.cgl.ucsf.edu/chimera/).

Heparin Affinity Chromatography. SmCB1 (10 μg) or synthetic peptides (50 nmol) were applied to a 1 mL HiTrap Heparin HP column (GE Healthcare Bio-Sciences) equilibrated with 25 mM sodium acetate, pH 5.5. A linear 0−1 M NaCl gradient was used to elute the bound material at a flow rate of 1 mL min^{-1}. Chromatography was monitored by measuring the absorbance at 280 nm.

Thermal Stability Assay. The thermal denaturation curves of SmCB1 were recorded in a thermofluor assay using the LightCycler 480 System

(Roche) and a thin-wall PCR plate format.[40] A temperature increment of 1 °C min^{-1} was applied. Samples (25 μL) contained 0.8 μg of SmCB1 in 0.1 M sodium acetate, pH 5.5, in the presence or absence of 25 μg mL^{-1} of 17 kDa heparin. Protein unfolding was monitored by measuring the fluorescence signal of the hydrophobic reporter dye Sypro Orange (Invitrogen) with excitation and emission wavelengths of 465 and 580 nm, respectively. Melting temperature (T_m) values were calculated using the first derivative method.[40]

■ ASSOCIATED CONTENT

Supporting Information. This material is available free of charge *via* the Internet at http://pubs.acs.org.

■ AUTHOR INFORMATION

Corresponding Author

*Tel: (+420) 220183356. Fax: (+420) 220183578. E-mail: mares@uochb.cas.cz.

■ ACKNOWLEDGMENT

This work was supported by grants 203/09/1585 from the Grant Agency of the Czech Republic (GACR), KJB400550516 and IAA400550705 from the Grant Agency of the Academy of Sciences of the Czech Republic (GAASCR), institutional research project Z40550506, the Academy of Science of the Czech Republic, and the Sandler Center for Drug Discovery (C.R.C. and M.H.). C.R.C. and M.H. were recipients of a NATO Collaborative Linkage Grant (NATO LST/CLG 980187). We thank Miroslava Blechová for peptide synthesis, Lucie Bednárová for CD spectroscopy, and Irena Pražáková for technical assistance.

■ REFERENCES

(1) Utzinger, J., N'goran, E. K., Caffrey, C. R., Keiser, J. (2010) From innovation to application: Social-ecological context, diagnostics, drugs and integrated control of schistosomiasis, *Acta Trop.* E-pub ahead of print; DOI: 10.1016/j.actatropica.2010.08.020.

(2) Gryseels, B., Polman, K., Clerinx, J., and Kestens, L. (2006) Human schistosomiasis. *Lancet 368*, 1106–1118.

(3) Caffrey, C. R. (2007) Chemotherapy of schistosomiasis: present and future. *Curr. Opin. Chem. Biol. 11*, 433–439.

(4) Delcroix, M., Sajid, M., Caffrey, C. R., Lim, K. C., Dvořák, J., Hsieh, I., Bahgat, M., Dissous, C., and McKerrow, J. H. (2006) A multienzyme network functions in intestinal protein digestion by a platyhelminth parasite. *J. Biol. Chem. 281*, 39316–39329.

(5) Caffrey, C. R., McKerrow, J. H., Salter, J. P., and Sajid, M. (2004) Blood 'n' guts: an update on schistosome digestive peptidases. *Trends Parasitol. 20*, 241–248.

(6) Dvořák, J., Mashiyama, S. T., Sajid, M., Braschi, S., Delcroix, M., Schneider, E. L., McKerrow, W. H., Bahgat, M., Hansell, E., Babbitt, P. C., Craik, C. S., McKerrow, J. H., and Caffrey, C. R. (2009) SmCL3, a gastrodermal cysteine protease of the human blood fluke Schistosoma mansoni. *PLoS Neglected Trop. Dis. 3*, e449.

(7) Sajid, M., McKerrow, J. H., Hansell, E., Mathieu, M. A., Lucas, K. D., Hsieh, I., Greenbaum, D., Bogyo, M., Salter, J. P., Lim, K. C., Franklin, C., Kim, J. H., and Caffrey, C. R. (2003) Functional expression and characterization of Schistosoma mansoni cathepsin B and its trans-activation by an endogenous asparaginyl endopeptidase. *Mol. Biochem. Parasitol. 131*, 65–75.

(8) Brady, C. P., Brinkworth, R. I., Dalton, J. P., Dowd, A. J., Verity, C. K., and Brindley, P. J. (2000) Molecular modeling and substrate specificity of discrete Cruzipain-like and cathepsin L-like cysteine proteinases of the human blood fluke Schistosoma mansoni. *Arch. Biochem. Biophys. 380*, 46–55.

(9) Hola-Jamriska, L., Dalton, J. P., Aaskov, J., and Brindley, P. J. (1999) Dipeptidyl peptidase I and III activities of adult schistosomes. *Parasitology 118* (Pt 3), 275–282.

(10) Caffrey, C. R., Mathieu, M. A., Gaffney, A. M., Salter, J. P., Sajid, M., Lucas, K. D., Franklin, C., Bogyo, M., and McKerrow, J. H. (2000) Identification of a cDNA encoding an active asparaginyl endopeptidase of Schistosoma mansoni and its expression in *Pichia pastoris*. *FEBS Lett. 466*, 244–248.

(11) Brindley, P. J., Kalinna, B. H., Wong, J. Y., Bogitsh, B. J., King, L. T., Smyth, D. J., Verity, C. K., Abbenante, G., Brinkworth, R. I., Fairlie, D. P., Smythe, M. L., Milburn, P. J., Bielefeldt-Ohmann, H., Zheng, Y., and McManus, D. P. (2001) Proteolysis of human hemoglobin by schistosome cathepsin D. *Mol. Biochem. Parasitol. 112*, 103–112.

(12) Williamson, A. L., Lecchi, P., Turk, B. E., Choe, Y., Hotez, P. J., McKerrow, J. H., Cantley, L. C., Sajid, M., Craik, C. S., and Loukas, A. (2004) A multi-enzyme cascade of hemoglobin proteolysis in the intestine of blood-feeding hookworms. *J. Biol. Chem. 279*, 35950–35957.

(13) Goldberg, D. E. (2005) Hemoglobin degradation. *Curr. Top. Microbiol. Immunol. 295*, 275–291.

(14) Sojka, D., Franta, Z., Horn, M., Hajdůšek, O., Caffrey, C. R., Mareš, M., and Kopáček, P. (2008) Profiling of proteolytic enzymes in the gut of the tick Ixodes ricinus reveals an evolutionarily conserved network of aspartic and cysteine peptidases. *Parasit. Vectors 1*, 7.

(15) Horn, M., Nussbaumerova, M., Šanda, M., Kovářová, Z., Srba, J., Franta, Z., Sojka, D., Bogyo, M., Caffrey, C. R., Kopáček, P., and Mareš, M. (2009) Hemoglobin digestion in blood-feeding ticks: mapping a multipeptidase pathway by functional proteomics. *Chem. Biol. 16*, 1053–1063.

(16) Abdulla, M. H., Lim, K. C., Sajid, M., McKerrow, J. H., and Caffrey, C. R. (2007) Schistosomiasis mansoni: novel chemotherapy using a cysteine protease inhibitor. *PLoS. Med. 4*, e14.

(17) Rawlings, N. D., Barrett, A. J., and Bateman, A. (2010) MEROPS: the peptidase database. *Nucleic Acids Res. 38*, D227–D233.

(18) Mach, L., Mort, J. S., and Glossl, J. (1994) Noncovalent complexes between the lysosomal proteinase cathepsin B and its propeptide account for stable, extracellular, high molecular mass forms of the enzyme. *J. Biol. Chem. 269*, 13036–13040.

(19) Yamamoto, Y., Kurata, M., Watabe, S., Murakami, R., and Takahashi, S. Y. (2002) Novel cysteine proteinase inhibitors homologous to the proregions of cysteine proteinases. *Curr. Protein Pept. Sci. 3*, 231–238.

(20) Wiederanders, B., Kaulmann, G., and Schilling, K. (2003) Functions of propeptide parts in cysteine proteases. *Curr. Protein Pept. Sci. 4*, 309–326.

(21) Roche, L., Tort, J., and Dalton, J. P. (1999) The propeptide of Fasciola hepatica cathepsin L is a potent and selective inhibitor of the mature enzyme. *Mol. Biochem. Parasitol. 98*, 271–277.

(22) Reis, F. C., Costa, T. F., Sulea, T., Mezzetti, A., Scharfstein, J., Bromme, D., Menard, R., and Lima, A. P. (2007) The propeptide of Cruzipain—a potent selective inhibitor of the trypanosomal enzymes Cruzipain and brucipain, and of the human enzyme cathepsin F. *FEBS J. 274*, 1224–1234.

(23) Fox, T., de, M. E., Mort, J. S., and Storer, A. C. (1992) Potent slow-binding inhibition of cathepsin B by its propeptide. *Biochemistry 31*, 12571–12576.

(24) Chagas, J. R., Ferrer-Di, M. M., Gauthier, F., and Lalmanach, G. (1996) Inhibition of cathepsin B by its propeptide: use of overlapping peptides to identify a critical segment. *FEBS Lett. 392*, 233–236.

(25) Lalmanach, G., Lecaille, F., Chagas, J. R., Authie, E., Scharfstein, J., Juliano, M. A., and Gauthier, F. (1998) Inhibition of trypanosomal cysteine proteinases by their propeptides. *J. Biol. Chem. 273*, 25112–25116.

(26) Horn, M., Dolečková-Marešová, L., Rulíšek, L., Máša, M., Vasiljeva, O., Turk, B., Gan-Erdene, T., Baudyš, M., and Mareš, M. (2005) Activation processing of cathepsin H impairs recognition by its propeptide. *Biol. Chem. 386*, 941–947.

(27) Pandey, K. C., Barkan, D. T., Sali, A., and Rosenthal, P. J. (2009) Regulatory elements within the prodomain of Falcipain-2, a cysteine protease of the malaria parasite *Plasmodium falciparum*. *PLoS One 4*, e5694.

(28) Korde, R., Bhardwaj, A., Singh, R., Srivastava, A., Chauhan, V. S., Bhatnagar, R. K., and Malhotra, P. (2008) A prodomain peptide of *Plasmodium falciparum* cysteine protease (falcipain-2) inhibits malaria parasite development. *J. Med. Chem. 51*, 3116–3123.

(29) Cygler, M., Sivaraman, J., Grochulski, P., Coulombe, R., Storer, A. C., and Mort, J. S. (1996) Structure of rat procathepsin B: model for inhibition of cysteine protease activity by the proregion. *Structure 4*, 405–416.

(30) Turk, D., Podobnik, M., Kuhelj, R., Dolinar, M., and Turk, V. (1996) Crystal structures of human procathepsin B at 3.2 and 3.3 Angstroms resolution reveal an interaction motif between a papain-like cysteine protease and its propeptide. *FEBS Lett. 384*, 211–214.

(31) Chowdhury, S. F., Sivaraman, J., Wang, J., Devanathan, G., Lachance, P., Qi, H., Menard, R., Lefebvre, J., Konishi, Y., Cygler, M., Sulea, T., and Purisima, E. O. (2002) Design of noncovalent inhibitors of human cathepsin L. From the 96-residue proregion to optimized tripeptides. *J. Med. Chem. 45*, 5321–5329.

(32) Li, Z., Hou, W. S., Escalante-Torres, C. R., Gelb, B. D., and Bromme, D. (2002) Collagenase activity of cathepsin K depends on complex formation with chondroitin sulfate. *J. Biol. Chem. 277*, 28669–28676.

(33) Almeida, P. C., Nantes, I. L., Chagas, J. R., Rizzi, C. C., Faljoni-Alario, A., Carmona, E., Juliano, L., Nader, H. B., and Tersariol, I. L. (2001) Cathepsin B activity regulation. Heparin-like glycosaminogylcans protect human cathepsin B from alkaline pH-induced inactivation. *J. Biol. Chem. 276*, 944–951.

(34) Caglic, D., Pungercar, J. R., Pejler, G., Turk, V., and Turk, B. (2007) Glycosaminoglycans facilitate procathepsin B activation through disruption of propeptide-mature enzyme interactions. *J. Biol. Chem. 282*, 33076–33085.

(35) Vasiljeva, O., Dolinar, M., Pungercar, J. R., Turk, V., and Turk, B. (2005) Recombinant human procathepsin S is capable of autocatalytic processing at neutral pH in the presence of glycosaminoglycans. *FEBS Lett. 579*, 1285–1290.

(36) Fairhead, M., Kelly, S. M., and van der Walle, C. F. (2008) A heparin binding motif on the pro-domain of human procathepsin L mediates zymogen destabilization and activation. *Biochem. Biophys. Res. Commun. 366*, 862–867.

(37) Cardin, A. D., and Weintraub, H. J. (1989) Molecular modeling of protein-glycosaminoglycan interactions. *Arteriosclerosis 9*, 21–32.

(38) Caffrey, C. R., Salter, J. P., Lucas, K. D., Khiem, D., Hsieh, I., Lim, K. C., Ruppel, A., McKerrow, J. H., and Sajid, M. (2002) SmCB2, a novel tegumental cathepsin B from adult *Schistosoma mansoni*. *Mol. Biochem. Parasitol. 121*, 49–61.

(39) Gandhi, N. S., and Mancera, R. L. (2008) The structure of glycosaminoglycans and their interactions with proteins. *Chem. Biol. Drug Des. 72*, 455–482.

(40) Uniewicz, K. A., Ori, A., Xu, R., Ahmed, Y., Wilkinson, M. C., Fernig, D. G., and Yates, E. A. (2010) Differential scanning fluorimetry measurement of protein stability changes upon binding to glycosaminoglycans: a screening test for binding specificity. *Anal. Chem. 82*, 3796–3802.

(41) Matulis, D., Kranz, J. K., Salemme, F. R., and Todd, M. J. (2005) Thermodynamic stability of carbonic anhydrase: measurements of binding affinity and stoichiometry using ThermoFluor. *Biochemistry 44*, 5258–5266.

(42) Hamed, R. R., Maharem, T. M., and El-Guindy, A. S. (1997) Proteoglycans from adult worms of *Schistosoma haematobium*. *J. Helminthol. 71*, 151–160.

(43) Choe, Y., Leonetti, F., Greenbaum, D. C., Lecaille, F., Bogyo, M., Bromme, D., Ellman, J. A., and Craik, C. S. (2006) Substrate profiling of cysteine proteases using a combinatorial peptide library identifies functionally unique specificities. *J. Biol. Chem. 281*, 12824–12832.

(44) Yamamoto, A., Tomoo, K., Hara, T., Murata, M., Kitamura, K., and Ishida, T. (2000) Substrate specificity of bovine cathepsin B and its inhibition by CA074, based on crystal structure refinement of the complex. *J. Biochem. 127*, 635–643.

(45) Pohl, J., Baudyš, M., Tomášek, V., and Kostka, V. (1982) Identification of the active site cysteine and of the disulfide bonds in the N-terminal part of the molecule of bovine spleen cathepsin B. *FEBS Lett. 142*, 23–26.

(46) Dolečková-Marešová, L., Pavlík, M., Horn, M., and Mareš, M. (2005) De novo design of alpha-amylase inhibitor: a small linear mimetic of macromolecular proteinaceous ligands. *Chem. Biol. 12*, 1349–1357.

(47) Cheng, Y., and Prusoff, W. H. (1973) Relationship between the inhibition constant (K1) and the concentration of inhibitor which causes 50% inhibition (I50) of an enzymatic reaction. *Biochem. Pharmacol. 22*, 3099–3108.

(48) Máša, M., Marešová, L., Vondrášek, J., Horn, M., Ježek, J., and Mareš, M. (2006) Cathepsin D propeptide: mechanism and regulation of its interaction with the catalytic core. *Biochemistry 45*, 15474–15482.

(49) MOE: Chemical Computing Group, 1010 Sherbrooke St.West, Suite 910, Montreal, Canada H3A 2R7; http://www.chemcomp.com.

(50) Labute, P. (2008) The generalized Born/volume integral implicit solvent model: estimation of the free energy of hydration using London dispersion instead of atomic surface area. *J. Comput. Chem. 29*, 1693–1698.